Frost, Ray L. and Bahfenne, Silmarilly (2010) *A Review of the Vibrational Spectroscopic Studies of Arsenite, Antimonite, and Antimonate Minerals.* Applied Spectroscopy Reviews: an international journal of principles, methods, and applications, 45(2). pp. 101-129.

A Review of the Vibrational Spectroscopic Studies of Arsenite, Antimonite, and Antimonate Minerals

Silmarilly Bahfenne and Ray L. Frost

Inorganic Materials Research program, School of Physical and Chemical Sciences, Queensland University of Technology, GPO Box 2434, Brisbane Queensland 4001, Australia

Abstract

This review focuses on the vibrational spectroscopy of the compounds and minerals containing the arsenite, antimonite and antimonate anions. The review collects and correlates the published data.

Key words: Arsenite, antimonite, antimonate, infrared spectroscopy, Raman spectroscopy

Arsenite, Antimonite and Antimonate Minerals

Introduction

Arsenic and antimony are found throughout the earth's crust as a variety of minerals, although not particularly abundant. It has been estimated that there are 2 grams of arsenic and 0.2 grams of antimony in every tonne of crustal rocks [1]. Many arsenic-bearing minerals associated with sulphides have been identified, such as arsenopyrite FeAsS, orpiment As_2S_3, and realgar α-As_4S_4. When these ores are oxidised, As_2O_3 is obtained as a by-product. Antimony also occurs with sulphur, Sb_2S_3 being the principal source. Many oxides have also been identified; valentinite Sb_2O_3 and cervantite $Sb^{3+}Sb^{5+}O_4$. Similar to As_2O_3, Sb_2O_3 is obtained during oxidation of sulphide ores [1-3].

Inorganic compounds containing Sb and As have found applications in many fields. As is used as monosodium methylarsenate ($NaMeHAsO_3$) in herbicides and pesticides, as arsenic acid ($AsO(OH)_3$) in wood preservative, and as sodium arsenite in aquatic weed control [1]. As also finds many uses in the pigment industry eg Paris green is copper acetoarsenite ($Cu_2(CH_3COO)(AsO_3)$) and Scheele's green is $CuHAsO_3$ [3]. The thin film industry has many arsenide semiconductors such as GaAs which are advantageous over Si semiconductors in that they have greater electron mobility and require less energy to induce conduction. InGaAs and AlGaAs are used in various lasers. Sb is used in a number of alloys due to its expansion on solidification; semiconductor grade AlSb, GaSb, and InSb are used in IR devices, diodes, and Hall-effect devices, and corrosion-resistant PbSb alloy is used in storage batteries to impart electrochemical stability and fluidity [1]. In the paint industry, antimony white is a substitute for white lead while antimony black or finely powdered antimony is used as a bronzing powder for metals and plaster [3]. Small amounts of arsenic and antimony are known to improve the properties of specific alloys.

Arsenic trioxide is the most important compound of As and occurs as arsenolite or claudetite (either I or II). When dissolved in neutral or acidic solutions it forms unstable arsenious acid, whose formula had been subject to much debate and is discussed later [1]. Salts are categorised into ortho-, pyro-, and meta-arsenious acids or H_3AsO_3, $H_4As_2O_5$, and $HAsO_2$ [3]. All but the alkali arsenites are insoluble in water; those of alkaline earth metals are less soluble

and those of heavy metals are insoluble [1]. The anions of meta-arsenites e.g. $NaAsO_2$ are linked by the corner O atoms forming a polymeric chain [4] (Fig. 1).

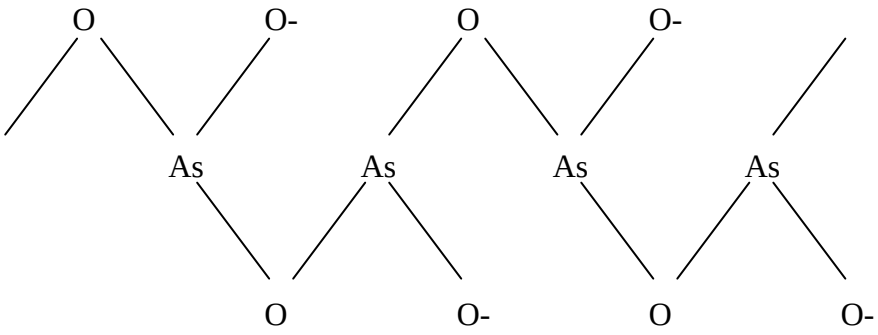

Fig 1. AsO_3 polymeric chain

The structure of arsenic trioxide has been reported to consist of As_4O_6 units present in solid, liquid, and vapour below 800°C. Vapour at 1800°C consists of As_2O_3 molecules [2]. Arsenic trioxide crystallises either as arsenolite (cubic) or claudetite (monoclinic) which dissolve slowly in water [5]. X ray analysis showed arsenolite having a molecular lattice of As_4O_6 units consisting of a three sided pyramid with an arsenic atom at the apex and three oxygen atoms at the base. Four of these pyramids are joined through the oxygen atoms forming an octahedron, with a cube of arsenic atoms contained within a structure that has been described as an adamantanoid cage [6]. Claudetite possesses alternating As and O atoms linked into sheets [2]. Claudetite is structurally related to $NaAsO_2$ in that it has a polymeric chain [4]. Claudetite is the thermodynamically stable form but conversion of arsenolite to claudetite is slow since the As-O-As bonds break and reform a new As_4O_6 unit. Conversion tends to be faster in the presence of heat or higher pH. Water also catalyses the conversion; it is thought that As-O bonds are protonated. It has been shown that the conversion from arsenolite to claudetite occurs at 125°C and greater [7]. It was thought that claudetite is less stable than arsenolite at temperatures below 50°C, however a more recent study solubility study showed claudetite to be less soluble and therefore more stable than arsenolite at temperatures up to 250°C [8]. The glassy form of As_2O_3 has a similar structure to claudetite, but its macromolecular structure is less regular [2].

Antimony trioxide exists as two crystalline forms which are insoluble in water, dilute nitric acid, and dilute sulphuric acid but is soluble in hydrochloric and organic acids and alkali

solutions. Salts can theoretically be categorised into ortho-, pyro-, and meta-antimonious acids or H_3SbO_3, $H_4Sb_2O_5$, and $HSbO_2$, although only the first form had been isolated [3]. Na_3SbO_3 was produced by fusing NaO and Sb_2O_3, and X-ray analysis showed it to be a tetramer. $NaSbO_2$, $NaSb_3O_5.H_2O$, $Na_2Sb_4O_7$ are also known [5]. The cubic senarmontite is stable at temperatures up to 517 °C whereas the orthorhombic valentinite exists at higher temperatures [2]. Valentinite consists of long double chains of SbO_3, where each Sb atom is connected to three O atoms, one of which bridges two Sb atoms forming a polymeric chain $[Sb_2O_3]_n$ [4]. The alternate Sb and O atoms are linked into bands [2]. Senarmontite consists of molecular units of Sb_4O_6 with each Sb atom having three Sb-O intramolecular bridging bonds and three Sb···O intermolecular bonds. Senarmontite slowly converts to valentinite upon heating.

Antimony pentoxide is almost insoluble in water but soluble in concentrated HCl [1]-[3]. Salts are poorly characterised but are categorised into hydrated and anhydrous salts, both of which do not have the SbO_3^{4-} anion in their structure [5]. Theoretically antimonic acids could be categorised, based on the different types of arsenic acids, into H_3SbO_4 (ortho), $H_4Sb_2O_7$ (pyro), or $HSbO_3$ (meta-antimonic acid) [3]. Hydrated salts such as $Li[Sb(OH)_6]$ and $Na[Sb(OH)_6]$ were all found to have the $[Sb(OH)_6]^-$ anion [2], which if dehydrated gives the edge-sharing polymeric octahedral $[SbO_6]_n^{n-}$. The presence of $[Sb(OH)_6]^-$ indicates that the parent acid is $HSb(OH)_6$ [5]. Solid antimonates have structures based on the SbO_6 octahedra, such as those having the ilmenite and trirutile structures [1]. The alkali metal salts have very low solubility.

Structural Studies of arsenite minerals

The arsenite group $[AsO_3]^{3-}$ is found in a pyramidal geometry due to the stereochemically active lone pair on the As atom. The anion can be found isolated or polymerised in a mineral structure. Reinerite $Zn_3(AsO_3)_3$ and finnemanite $Pb_5(AsO_3)_3Cl$ have the anion isolated whereas arsenites polymerised via their vertices can be found in paulmooreite $Pb_2As_2O_5$ and ludlockite $PbFe_4(As_5O_{11})_2$. As mentioned above the synthetic $NaAsO_2$ has the anions linked in a polymeric manner. The polymerisation of the arsenite group resulting in an infinite chain of $[AsO_2]_n^{n-}$ is termed a catena-arsenite chain [9]. This chain is also found in the minerals trippkeite $CuAs_2O_4$ and leiteite $ZnAs_2O_4$, and in the synthetic $Pb(AsO_2)Cl$ and $Pb_2(AsO_2)_3Cl$.

Many structural studies have been conducted on the minerals mentioned above. Leiteite $ZnAs^{3+}{}_2O_4$, although being an analogue of trippkeite $CuAs^{3+}{}_2O_4$, was discovered to have a different structure type [10]. Each Zn atom is found in an open tetrahedral geometry, with arsenite chains flanking each layer on either side. The layers are cross-linked through bridging As – O bonds that are longer and therefore weaker than the non-bridging As – O bonds. The average Zn – O distance in the sheet is 1.986 Å with O – Zn – O angles ranging from 102 – 116°. Within the arsenite chains are two groups of trigonal pyramidal $[AsO_3]^{3-}$ which differ slightly in their average As – O distances (1.79 and 1.78 Å) and O – As – O angles (95.5 and 95.8°). Each As has two shorter non-bridging bonds (1.76 and 1.73 Å) with O and one longer bridging bond (about 1.80 Å). Furthermore, the lone electron pair on As enables three extra O atoms at distances from 2.84 to 3.34 Å to create weak bonds with it, creating the trigonal pyramidal geometry and the approximate site symmetry m(C_s). Trippkeite, on the other hand, has its cations in an octahedral geometry.

Reinerite $Zn_3(AsO_3)_3$ occurs in the same horizon of oxidation zone as leiteite [11]. A $[Zn_2O_6]^{8-}$ dimer is formed by edge-sharing of two ZnO_4 tetrahedra. Edge-sharing causes distortion within the tetrahedron, demonstrated by the distance between the two shared O atoms (2.709 Å) being shorter than the average tetrahedral edge distance (3.173 Å) and the O – Zn – O angle (86.1°) being smaller than the average tetrahedral angle. Between two dimers sharing their O atoms are AsO_3 groups in trigonal pyramid geometry with point symmetry m. The average As – O bond length is 1.769 Å and O – As – O is 97.6°. The bond length is in good agreement with the As^{3+} – O distance of synadelphite $Mn_9(OH)_9(H_2O)_2(AsO_3)(AsO_4)_2$ but is considerably lower than that of asbecasite $Ca_3Ti(As_3SiBeO_{10})_2$ and finnemanite $Pb_5Cl(AsO_3)_3$. Unlike leiteite, no additional O atoms are weakly bonded to the As^{3+} within 3.5 Å. Bonded to one of the O atoms on either side of the dimer is another Zn atom which forms a ring with other three Zn atoms, each of which is a tetrahedral sharing O corners forming double chains. These tetrahedral also show angular distortion, with the O – Zn – O angle ranging from 99.9 to 119.6°. The arsenite groups strengthen the three-dimensional framework by causing two adjacent double chains with a corner of the dimer. Each O atom is being shared by two Zn atoms and one As atom.

Paulmooreite $Pb_2[As_2O_5]$ contains $[As^{3+}{}_2O_5\ ]^{4-}$ doublets which share a common O atom forming dimers whose triangular bases are oriented nearly normal to each other [12]. Each Pb accepts four O atoms in a distorted tetragonal pyramid with bond distances ranging from 2.26 –

2.55 Å. Average Pb^{2+} – O distances of both Pb atoms in the asymmetric unit are in agreement with minerals such as alamosite $Pb^{2+}SiO_3$ and larsenite $Pb^{2+}[ZnSiO_4]$. The O atom shared by the two As atoms further receives an extra bond from a Pb; this Pb – O bond is 2.94 Å, outside the range mentioned above. The other Pb accepts two additional longer bonds with O of distance 2.80 and 3.06 Å. As^{3+} – O average distances of 1.77 and 1.78 Å also compare well to those of magnussonite $Mn^{2+}{}_5As^{3+}{}_3O_9(OH,Cl)$, stenhuggarite $CaFe^{3+}(As^{3+}O_2)(As^{3+}Sb^{3+}O_5)$, armangite $Mn_{26}As^{3+}{}_{18}O_{50}(OH)_4(CO_3)$.

Vibrational Spectroscopy of Arsenic and Antimony Trihalides

The vibrational spectra of the C_{3v} gaseous and liquid halides of As^{3+} and Sb^{3+} have been recorded. The four fundamentals which are both Raman and infrared active are shown in the following table. Wavenumber positions vary slightly between sources [2,13].

An attempt at building a database of Raman spectra of minerals was published [14]. It relied on the existence of the totally symmetric vibrational mode which is usually observed as the strongest band in the characteristic spectral region. This mode corresponds to the most covalentic chemical bond of the anionic unit. It categorised the minerals into several groups, one of which included minerals having a $(XO_3)^{n-}$ unit such as carbonates and arsenites. The inclusion of arsenite minerals in this category must be examined carefully. The existence of a polymeric chain of AsO_3 in some minerals means that the vibrating unit is not isolated and may not vibrate like one would expect a $(XO_3)^{n-}$ unit possessing a D_{3h} free symmetry. Another category included minerals having a polymer of units in which corner O atoms are shared. Therefore two totally symmetric bands are expected; one corresponding to bonds belonging to non-bridging O atoms, and the other to bridging O atoms. The wavenumber of the latter is usually lower than the former. The relative intensities of the two bands vary depending on the ratio of non-bridging O to bridging O atoms. Some arsenite minerals such as leiteite may be better suited to fall under this category.

Positions and intensities of infrared absorption bands have been reported for As_2O_3 ,Sb_2O_3 and Sb_2O_5 [15] and they are summarised in the following table. The samples were pure inorganic salts and were ground to a powder and analysed as a Nujol mull. The type of As_2O_3 was not mentioned (claudetite or arsenolite). No band assignments were made.

Matrix Isolation Spectroscopy of Gaseous Arsenites and Antimonites

The infrared spectra of high temperature ternary oxides isolated in N_2 matrix have been reported [16]. Spectra of $NaAsO_2$, $NaSbO_2$, and $KSbO_2$ were obtained by vaporisation from alumina tubes and the vapours collected on CsI surface window maintained at 12K. The above spectra were compared to those obtained by vaporising a 1:1 mixture of M_2CO_3 with As_2O_3 or Sb_2O_3. Using both techniques, the spectrum of $NaAsO_2$ displayed three bands at 868, 853, and

418 cm^{-1} and $NaSbO_2$ at 767, 746, and 340 cm^{-1}. The three bands were observed in all spectra containing either of the two oxyanions while varying the cation (Na, K, Rb, and Cs). It is noted that the band with highest absorption is located at the second highest wavenumber i.e. 853 cm^{-1} for $NaAsO_2$ and 746 cm^{-1} for $NaSbO_2$. The band at the highest wavenumber (868 cm^{-1} for $NaAsO_2$ and 767 cm^{-1} for $NaSbO_2$) has a less intense absorption. Therefore the less intense band is assigned to the A_1 symmetric stretch and the more intense band to B_2 antisymmetric stretch. It is interesting to note that the antisymmetric mode lies below the symmetric mode, instead of the other way around observed in the case of PO_2^- and VO_2^-. In the molecules above, the cation coordinates to the anion via two equivalent oxygen atoms (Fig 2). The C_{2v} ring structure of the molecules was confirmed by ^{18}O enrichment; the spectrum of ^{18}O enriched $CsAsO_2$ consisted of nine bands as a result of each of the three bands previously observed splitting into a triplet. Each triplet has a ratio of 1:2:1 characteristic of a species with two equivalent O atoms. The spectrum of ^{18}O enriched $KSbO_2$ is qualitatively similar to that of $CsAsO_2$.

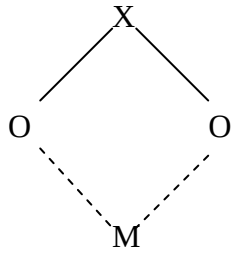

Fig 2. XO_2^- coordination to cation

The above study reported bands at 863, 851, and 393 cm^{-1} for $CsAsO_2$ and 764, 745, and 339 cm^{-1} for $KSbO_2$. The reproducibility of the band positions is demonstrated by a different study that reported the same band positions [17]. Both studies also report the O-As-O angle to be 115° and the O-Sb-O angle to be 106°. Results are tabulated below in Table 4.

Spectroscopy of As_2O_3

Many studies have reported IR and Raman spectra of arsenolite (As_4O_6) in its solid, hydrated, and gas phases [18,19,21]. A theoretical study has also been published [6,21]. Table 5 summarises the results. Band assignments vary between authors.

Szymanski [18] wrote that the vibrations of solid As_4O_6 can be described as those of the AsO_3 pyramid and two vibrations of the As_4O_6 tetrahedron as a whole. Band assignment for As_4O_6

was based on that of P_4O_6 since they both possess a T_d point symmetry, whereas the band assignment for AsO_3 was based on the SeO_3^{2-} ion since mass of Se is very similar to that of As and SeO_3^{2-} and AsO_3 have C_{3v} symmetry. IR bands at 845 and 800 cm^{-1} (Raman at 830 and 785 cm^{-1}) were assigned to As-O antisymmetric and symmetric stretches respectively. The IR inactive symmetric breathing vibration of the As_4O_6 tetrahedron was observed in the Raman spectrum at 555 cm^{-1}. Bands at 475, 375, and 275 cm^{-1} were assigned to the deformation mode of the AsO_3 pyramid (first two) and deformation of As_4O_6 tetrahedron respectively. Although no assignment was made, Loehr and Plane reported similar Raman bands for solid As_4O_6 at 782, 561, 473, 372, 269, and 240 cm^{-1}[19].

Lezal and Konak [26] have reported IR bands at 258, 346, 482 (strong), and 808 cm^{-1} (very strong), and is supported by calculated values [6,21]. The above bands agree with those observed by Szymanski [18]. Assignment of the bands is as follows; 808 and 482 cm^{-1} are As-O-As stretches, 346 cm^{-1} is the As-O-As bend, and 258 cm^{-1} is the As-O-As wag [6].

Beattie [25] has reported a gas-phase Raman spectrum of As_4O_6, which has the same 'cage' structure in the vapour phase. Bands at 492 (weak) and 556 cm^{-1} (very strong) are assigned to symmetric As-O-As stretch, and the symmetric As stretch is found at 381 cm^{-1} (very strong) [21]. These values are in close agreement to calculated ones [6,21]. Raman spectrum of powder As_4O_6 shows absorption at almost the same wavenumbers (370, 470, and 560 cm^{-1}). In a different theoretical study [6], GAUSSVIEW visualisation program was used to determine the predominant type of motion (As-O-As stretch, bend, or wag). In this study bands observed by Beattie at 556, 492, and 409 cm^{-1} are assigned to As-O-As stretches, and bands at 381 and 184 cm^{-1} are assigned to As-O-As bends. Other gas-phase and solid Raman spectra [27,29] agree with Beattie's results.

Solutions of As_4O_6 are thought to contain $As_4O_6 \cdot xH_2O$ units and a small portion of $As(OH)_3$ [18]. As-O antisymmetric and symmetric stretches of $As_4O_6 \cdot xH_2O$ were observed at 800 and 750 cm^{-1}, confirmed by the fact that the two bands did not shift in position upon addition of D_2O. The strong intensity of these bands supports the theory that the hydrate is present in higher concentrations than other forms of arsenious acid. OH vibrations were observed at 3650, 3570, 3520 (stretches), and 1600 cm^{-1} (bend). Bands at 3650, 3570, and 1600 cm^{-1} were assigned to the dissociated H_2O bound to As_4O_6, most likely located at the apex of the AsO_3 pyramid. The assignment was made based on the fact that the above bands show only a slight

shift in wavenumbers to those observed for water vapour (3750, 3650, and 1590 cm^{-1}). The band at 3520 cm^{-1} is assigned to the OH stretch of $As(OH)_3$. Other bands of $As(OH)_3$ were predicted by assuming a C_{3v} symmetry; two As-O stretches nearly coincidental with each other occurring as a broad peak at 690 cm^{-1} which appears in both Raman and IR spectra.

Identification of the various forms of arsenious acid were based on selecting related series of bands which retain the same intensity relative to each other with varying experimental conditions.

The O=As-OH form of the acid was eliminated because if it existed medium IR bands at 1250 and 900 cm^{-1} and a series of weak bands at 2800 – 2400, 2350 – 1900, and 1720 – 1600 cm^{-1} would be observed. The $(HO)_2As\text{-}O\text{-}As(OH)_2$ form, which could form from two $As(OH)_3$ molecules, was also eliminated on the basis that the IR spectrum displayed only a strong band in the 3600 – 2800 cm^{-1} instead of two OH bands near 3000 and 2500 cm^{-1} [20] which is expected of a group with the formula $RM(OH)_2$. The separation of the OH bands occurs due to the coupling through the heavy central atom such as S, Se, and P.

Raman Investigation into Arsenite Speciation in Aqueous Solutions

Solubility of As_4O_6 is known to increase by addition of a base. Loehr and Plane prepared solutions containing varying compositions of OH^- and As^{3+} ($[As^{3+}] + [OH^-] = 8.0$ M, and ratio $R = [OH^-] / [As^{3+}]$ ranged from 3.5 to 15) and recorded their Raman spectra [19]. The study concluded that there are at least three As^{3+} species which give rise to its own Raman spectrum.

$As(OH)_3$ gives rise to bands at 710 and 655 cm^{-1} indicating its symmetric and antisymmetric As-(OH) stretches respectively. These bands were observed in solutions saturated with As_4O_6 (pH = 0 – 4) and in solutions where the ratio $[OH^-]/[As^{3+}] = 3.5$ and shift by about 20 cm^{-1} in D_2O solution. Bands around this position were observed in another study [18] although broader and overlapping, and confirms its assignment to As-OH of $As(OH)_3$. Both studies reported $As(OH)_3$ to have C_{3v} symmetry since the symmetric stretch is found at a higher wavenumber than the antisymmetric stretch. Furthermore many AsX_3 such as structures where X = any halide have been shown to have a C_{3v} symmetry as well.

$AsO(OH)_2^-$ is formed as more base is added according to the reaction $As(OH)_3 + OH^- \rightarrow AsO(OH)^{2-} + H_2O$. Bands corresponding to this species are observed in solutions where the ratio $[OH^-]/[As^{3+}] = 4$. As-O stretch is assigned to a band at 790 cm^{-1}, while symmetric and antisymmetric stretches of As-OH to 570 and 610 cm^{-1} respectively. The 790 cm^{-1} band did not shift in position in D_2O solution while the bands around 600 cm^{-1} did. This species, possessing a mirror plane, belongs to C_s symmetry and hence would give six Raman-active bands. Only two out of three bending modes were observed at 320 and 370 cm^{-1}.

AsO_3^{3-} appeared in solutions with high ratios of $[OH^-]/[As^{3+}] \approx 15$. A band 752 cm^{-1} is assigned to As-O symmetric stretch whereas the band 680 cm^{-1} is assigned to the antisymmetric stretch. It also belongs to C_{3v} symmetry which explains the reason why the symmetric stretch occurs at a higher wavenumber than the antisymmetric stretch. A bending mode at 340 cm^{-1} was also observed. $AsO_2(OH)^{2-}$ is also thought to exist as a product of stepwise dissociation of $As(OH)_3$ in solutions where $[OH^-]/[As^{3+}] \approx 6$. Since it has C_s symmetry, the antisymmetric As-O stretch is expected to occur at a higher wavenumber than the symmetric stretch. The symmetric As-O stretch is expected to appear midway between the observed positions of $AsO(OH)_2^-$ and AsO_3^{3-} (790 and 752 cm^{-1} respectively) and the antisymmetric around 800 cm^{-1}. The expected positions match the observed intensities in this region.

A theoretical study calculated structures, stabilities and the vibrational spectra of $As(OH)_3$ and its anions in solution, and of the oligomers [21]. The programs GAMESS and GAUSSIAN94 were implemented to obtain IR wavenumber and intensities, and Raman wavenumbers. The O=As-OH form was determined not to be stable in aqueous solution since its reaction with H_2O to form $As(OH)_3$ is exothermic by over 40 kcal/mol. $HAsO(OH)_2$ was also found to have a higher energy than $As(OH)_3$, therefore the stable neutral monomer is expected to be $As(OH)_3$. The calculated stretching wavenumbers of $As(OH)_3$ agree with the experimental values determined by Loehr and Plane while some calculated wavenumbers of $AsO(OH)_2^-$, $AsO_2(OH)^{2-}$, and AsO_3^{3-} do not agree closely with experimental values.

A later study [22], which utilised methods thought to improve accuracy of electron correlation and incorporation of anharmonic and hydration effects semi-quantitatively found that $AsO(OH)_2^-$ can be better modelled in terms of the ion pair $AsO(OH)_2^- \ldots Na^+$. The calculated wavenumbers for this ion pair are 836, 606, and 530 cm^{-1} which are in better agreement with

experimental wavenumbers of 790, 610, and 570 cm^{-1}. This indicates that ion-pairing may be important for the formation of $AsO(OH)_2^-$. The new calculated wavenumbers for $AsO_2(OH)^{2-}$ and AsO_3^{3-} still do not agree closely with experimental data. The authors noted that it is difficult to apply their technique to anions with larger charges because the hydration and counter-ion effects are expected to be much larger, and because the experimental data are less certain.

Another Raman study [23] in the speciation of arsenite in aqueous solution confirmed the results obtained by Loehr and Plane. A diagram constructed using data from an earlier study [24] shows the distribution of arsenite species as a function of pH at 25°C and 1 bar is also included which allows the confirmation of the species present at a certain pH. Broad bands near 600 and 800 cm^{-1} corresponding to $AsO_2(OH)^{2-}$ and AsO_3^{3-} are observed at pH=13.2. At pH=12.6 the above bands become narrower indicating the dominance of $AsO_2(OH)^{2-}$, the disappearance of the lower wavenumber shoulder of the 800 cm^{-1} band indicates absence of 750 cm^{-1} band corresponding to AsO_3^{3-}. Spectra at pH=10.5 show an intense band at 790 cm^{-1} and therefore $AsO(OH)_2^-$ to be most dominant. A small proportion of $As(OH)_3$ is also present at this pH visible by the weak band at 700 cm^{-1}. At pH=8.5 and lower, the dominant species is $As(OH)_3$ seen by a strong band at 700 cm^{-1} with a shoulder at 650 cm^{-1} and the less dominant species is $AsO(OH)_2^-$. The arsenite species determined to be present at a given pH based on the spectra agree closely with the diagram.

Existence of Polymeric Species in Aqueous Solutions

Loehr and Plane also conducted an investigation into the existence of polymeric As^{3+} but detected no spectral changes with dilution and up to 80°C. A more recent study by Pokrovski showed that at 275°C, pH $\leq$ 6, and As concentration up to 1 mol/kg, the symmetric stretching mode of $As(OH)_3$ at 700 cm^{-1} shifts by 5 – 10 cm^{-1} and the antisymmetric stretch at 650 cm^{-1} broadens slightly due to weakening of hydrogen bonds with increasing temperature [8]. Over 1 M, additional bands appear at about 520 and 380 cm^{-1} which increase in intensity with increasing As concentration and temperature. These bands are assigned to the formation of As-O-As bonds, because these bands are also observed in amorphous and molten As_2O_3 which are both known to possess As-O-As chains. The 380 cm^{-1} band is assigned to the symmetrical vibration of As_4O_6 tetrahedron because it was also observed in gas-phase and

powder spectra of As_4O_6 in a separate study by Beattie [24]. A theoretical study [6], however, assigns this band to As-O-As bend.

A number of As hydroxide and oxide oligomers structures are envisaged and their normal modes are calculated [21]. The energy differences for various polymerisation reactions were also calculated. The condensation of $3As(OH)_3$ is shown to give $As_3O_3(OH)_3$ and $3H_2O$, is favoured entropically and will become more favourable with increasing temperature. For $As_3O_3(OH)_3$ bands are calculated at 378, 437, 512, and 665 cm^{-1}. The broad band centred at 520cm^{-1} (which probably constitutes several bands including one near 437cm^{-1}) observed at high temperatures by Pokrovski is thus assigned to $As_3O_3(OH)_3$ symmetric bridging O stretch, whereas the band at 665 cm^{-1} corresponds to symmetric As-OH stretch (which seems to occur around 650 – 700 cm^{-1} in both monomers and all oligomers according to the calculations). This study noted that bands near 370 cm^{-1} (such as that observed by Pokrovski) is probably characteristic of oligomers mainly involving symmetric As motion but highlighted that it does not correspond to As_4O_6; because the broad band around 700 cm^{-1} indicates that the oligomeric species possesses As-OH groups. It seems that $As_3O_3(OH)_3$ is the most probable oligomeric species in solution. The calculated and experimental vibrational wavenumbers of $As_3O_3(OH)_3$ are summarised in the following tables.

The species $As_3O_3(OH)_3$ is also thought to exist in glassy As_2O_3 [26]; experimental data shows a band at 805cm^{-1} and a broad band centred around 650 which probably constitutes the calculated 633 and 665 cm^{-1} bands.

Raman spectra of aqueous arsenic solutions of varying concentration and temperature were recorded [30]. At low concentrations ($0.02 \leq m_{As} \leq 0.33$ mol/kg), 20°C, and at pH 0 – 8 the spectra appear the same; polarised sharp band at 700 cm^{-1} and depolarised shoulder at 650 cm^{-1} very similar to those observed by Loehr and Plane. At pH > 8 $AsO(OH)_2^-$ appears as seen by new bands appearing at 600 and 790 cm^{-1}. Neutral arsenic solutions at low and medium (~0.5 mol/kg) concentrations were also studied under varying temperatures up to 275°C. Both bands only shift by about 5 cm^{-1} towards the lower wavenumber as temperatures increase indicating that only the monomer $As(OH)_3$ dominates. At higher concentrations (1 mol/kg) the sharp band starts to broaden and split into two bands at 696 and 669 cm^{-1} at 275°C, which is thought to have been caused by the formation of a dimeric hydrated arsenic species which consists of two $As(OH)_3$ molecules held together by

hydrogen bonding. The splitting increases as concentration increases to 2 mol/kg at temperatures 175 – 275 °C. A new polarised band is observed at 525 cm^{-1}. At even higher concentrations (4.1 and 5.2 mol/kg) this new band increases in intensity with increasing concentrations and temperature. Similar behaviour is observed in a polarised band at 380 cm^{-1} which started to appear at 4.1 mol/kg. The band at 525 cm^{-1} is similar to that observed in fused (at 275 °C) and amorphous (at 20 °C) arsenic oxide, so it was assigned to As-O-As bond. Possible polymeric species envisaged by the author with the aid of molecular dynamic calculations include a dehydrated dimer $As_2O(OH)_4$, $As_3O_6(OH)_3$, $As_6O_6(OH)_6$, and As_4O_6. The presence of the 380 cm^{-1} band in highly concentrated As solutions is similar to that observed in arsenolite and gas-phase As_4O_6 but not claudetite, so it probably indicates the formation of As_4O_6 and corresponds to As-O-As bend as described by Jensen et al. [6].

It was noted that in highly concentrated solutions intensity of the As-O-As vibration is much higher than that of As-OH vibration, and the difference gets higher with increase in temperature. At higher temperatures, the increase in As-O-As vibration intensity also gets steeper with increase in As concentration. The authors suggested that this phenomenon is due to the formation of small polymers (dimers or trimers) in the 2 mol/kg solution and bigger polymers, which require expulsion of more water molecules, in the more concentrated solutions.

Preparation of Arsenites

Szymanski [18] had observed that when alkali halides are present in arsenic trioxide or arsenic trichloride solutions, arsenites of the form M_3AsO_3, or ortho arsenites, are produced. The same product is also obtained by reacting an alkali meta arsenite e.g. $KAsO_2$ with water in the presence of alkali halide. The reaction is thought to start by an As-OH group being attacked by the alkali halide MX to produce HX and an As-OM group. Two As-OM groups give an As-O-As bridge. The formation of an ortho arsenite requires three such bridges.

Alkali metal arsenites such as $NaAsO_2$, $KAsO_2$, and $RbAsO_2$ have been synthesised by solid state reaction using a 1:1 mixture of the elemental alkali metal and As_2O_3 under Ar gas [31]. It is heated to 500 °C at a rate of 50 °C/hour and then cooled afterwards at a rate of 5 °C/hour to room temperature. $Cs_3As_5O_9$ was synthesised in a similar fashion except a cooling rate of 25 °C/hour was used. Terminal As-O bond was found to be shorter than bridging As-O bond

in the above compounds. The bond angles of O_t-As-O_b are around about 4° greater than those of O_b-As-O_b.

Other synthetic minerals that have been prepared include $Pb(AsO_2)Cl$, $Pb_2(AsO_2)_3Cl$, and $Pb_2As_2O_5$ [32]. $Pb(AsO_2)Cl$ was prepared by mixing As_2O_3 and $PbCl_2$ in a ratio of 1:2 in a teflon-coated vessel which was filled with a 1 M acetic acid solution. It was heated to a temperature ranging from 300 to 500 K and left to react for 10 days. The same procedure was implemented to prepare $Pb_2(AsO_2)_3Cl$ except that a mixture of PbO and $PbCl_2$ in a 10:1 weight % ratio was used instead of pure $PbCl_2$. The result was $Pb_2(AsO_2)_3Cl$ and $Pb_2As_2O_5$ in a weight ratio of 1:50. Unfortunately no vibrational spectroscopy was performed on these synthetic samples.

Copper arsenite has been prepared for the purpose of application in the purification of copper electrolyte [33]. As_2O_3 is first dissolved in NaOH solution, in which $CuSO_4 \cdot 5H_2O$ is dissolved later. The reaction was carried out at 20°C. The optimum molar ratios n OH^-:n As and M (Cu): M (As) were both found to be 2:1 and the NaOH concentration 1 mol/L. H_2SO_4 was used to adjust the pH of the reaction, and at pH 4 the product is yellow-green in colour while at pH 6 the product is green. The two showed different XRD patterns. The former product was $Cu(AsO_2)_2$ while the latter was only labelled copper arsenite X since the structure is unknown.

Pertlik [34] has previously prepared $CuAs_2O_4$ or trippkeite by hydrothermal route. As_2O_3 and CuO are placed in an autoclave (mole ratio 1:1, total mass 0.5 g) along with the solvent which could be CH_3COOH or H_2O. If CH_3COOH is used the temperature range should be 200 – 250°C, but other products are formed at this temperature including Cu and Cu_2O. If H_2O is used trippkeite forms above 100°C and no other product would form below about 200 °C. In either case the reaction is left for 48 hours. The product is then mixed with 500 mL H_2O and placed on a water bath at a temperature of 60°C and left for two hours to get rid of all water-dissolvable compounds.

Scheele's green, $Cu_3(AsO_3)_2 \cdot 2H_2O$ or copper ortho-arsenite, and Paris green, $Cu_4(AsO_2)_6(CH_3COO)_2$ or copper aceto meta arsenite, were used as pigments in ancient artworks but they have also been prepared in the laboratory [35]. Scheele's green was

prepared according to the following reaction $3Cu(OH)_2 + As_2O_3 \rightarrow Cu_3(AsO_3)_2 \cdot 2H_2O$ or $3CuO + 3CuCl_2 + As_2O_3 + 2H_2O + 6NaF \rightarrow Cu_3(AsO_3)_2 \cdot 2H_2O + 3CuF + 6NaCl$.

Paris green is obtained by precipitation from a solution containing copper ion, acetate ion and As_2O_3 followed by evaporation of acetic acid. The reaction is as follows, $4\ CuCl_2 + 8(CH_3COO)Na + 3As_2O_3 + 3H_2O \rightarrow Cu_4(AsO_2)_6(CH_3COO)_2 + 6CH_3COOH + 8NaCl$.

In a late study by Pertlik [34] Paris green was prepared by a hydrothermal route; As_2O_3 and CuO are placed in an autoclave (mole ratio 1:1, total mass 0.5 g) along with CH_3COOH. The temperature range should be 100 – 200°C, left for 48 hours. The product is mixed with 500 mL H_2O and placed on a water bath at a temperature of 60°C and left for two hours to get rid of all water-dissolvable compounds. The study found that in neutral or basic solutions ortho salts are formed while the meta salts precipitate in acidic solutions. Zinc meta-arsenite was also prepared by the same author and also in another study by Avery [36]. As_2O_3, $ZnCl_2$, CH_3COONa, and glacial acetic acid were dissolved in water and a current of air is passed through to cause evaporation and thus precipitation of $Zn(AsO_2)_2$. $LiAsO_2$ has also been prepared by solid state reactions [37]. As_2O_3 is mixed with LiOH, $LiNO_3$, Li_2CO_3 or Li_2O with molar ratio of 1:1 and the mixture ground well. The mixture is placed in a porcelain crucible and into a furnace that has been pre heated to 100°C. The temperature was kept at 100°C for an hour, then elevated to 400°C (or 600°C for Li_2CO_3) and kept at that temperature for 10 hours. The colour of the product is white.

Spectroscopy of Synthetic Arsenite

Szymanski [18] wrote that the As-O-As bridge, whether in the ortho or meta form, is identified by a strong band at 570 cm^{-1}, based on the appearance of a band at the same wavenumber for compounds with a Se-O-Se bridge. The As-O-As deformation modes appear at 280 cm^{-1} or, as described by Jensen et al. [6], the As-O-As wag.

Table 8 below lists bands observed in the powder spectra of metal arsenites. The Raman bands may only represent a minimum number, since strong Raman lines were difficult to obtain. The AsO_3^{3+} ion is thought to be octahedral; octahedral ions exhibit the highest wavenumber band in

both IR and Raman spectra at positions very near to each other which, in this case, is probably the peak at 670 cm^{-1}. Also, spectra of salts with a perovskite structure (where the metal atom is surrounded by six O atoms) such as $CaZrO_3$ also exhibit bands at 670, 580, 320, and 280 cm^{-1}, and other M-O groups with a coordination number of six exhibit bands at very similar positions. As mentioned above, the band around 560 cm^{-1} indicates bridging As-O-As groups of ortho and meta arsenites while a band near 280 cm^{-1} in spectra of ortho arsenites indicate the deformation mode of the As-O-As bridge.. The band at 820 cm^{-1} observed in the IR spectrum of meta arsenites indicate As-OM groups. No further band assignment was made concerning the metal arsenites. It may be useful to obtain a better powdered sample.

Another study [15] reported the infrared spectrum for $NaAsO_2$ which showed bands at 697 (very strong, broad), 748 (medium), 775 (weak, shoulder), 833 (strong, sharp), 848 (strong, sharp), 1420 (very weak), 1460 (medium, sharp), 3450 cm^{-1} (weak, broad).

The Raman spectra from the study by Röhr [31] were not presented in detail, the study only mentioned the highest wavenumbers; 836 cm^{-1} for $KAsO_2$, 832 cm^{-1} for $RbAsO_2$, and 836 cm^{-1} for $Cs_3As_5O_9$ which can be assigned to the stretching of terminal As-O. These bands lie above those assigned to the stretch of the bridging As-O.

Paris green and Scheele's green's Raman spectra have been recorded and the band positions are tabulated below [38].

Spectroscopy of Arsenite Minerals

A single crystal of cafarsite, $Ca_8(Ti, Fe, Mn)_{6-7}(AsO_3)_{12}\bullet 4H_2O$, has been analysed using polarised Raman spectroscopy and the results compared with other metal oxides to achieve assignment of bands [39]. It is of cubic symmetry of space group Pn3. The As atoms are at the apices of a trigonal pyramidal coordination but the pyramids are not connected to each other. There are two different Fe and Ca atoms. The two Ca are coordinated. Polarised and cross-polarised spectra of the 001, 100, 010, and 111 faces were obtained and the spectra were identical. For symmetric pyramidal shapes four fundamental wavenumbers are expected which consist of a degenerate stretch and a degenerate deformation. Symmetric stretch (ν_1) and out-of-plane deformation (ν_2) are expected to be polarised and the antisymmetric stretch (ν_3) and deformation (ν_4) should be depolarised. The study compared vibrations of the AsO_3 of

cafarsite to those of AsF_3 and noted that differences in band positions between the two are mainly due to the state in which the spectra were obtained (AsF_3 was in liquid state) and the difference of atomic weight between O and F. The authors wrote that bands of AsF_3 (274, 343, 644, and 715 cm^{-1}) are similar to those of AsO_3 (258, 319, 721, and 763 cm^{-1}), keeping in mind that the 763 and 319 cm^{-1} bands should be completely polarised. The Fe-O vibrations were assigned based on hematite (Fe_2O_3) vibrations, those of Ca-O based on CaO, those of Mn-O based on hausmannite ($Mn^{2+}Mn^{3+}{}_2O_4$) and pyrolusite (MnO_2), and those of Ti-O based on anatase TiO_2.

Raman Investigations of Antimony Speciation in Aqueous Solutions

$Sb(OH)_3$ is found to be the main species responsible for Sb transport under moderately acidic to near neutral conditions while $Sb(OH)_4^-$ is predominant over pH 10 in sulphide-poor solutions. In sulphide-rich, near neutral to alkaline solutions thioantimony species may be important for Sb transport. However $Sb(OH)_3$ is primarily responsible for hydrothermal transport of Sb especially at temperatures above 200 – 250°C even in sulphide-rich systems [40]. The solubility of Sb^{3+} and Sb^{5+} increases with solution acidity [41]. Sb_2O_3 is dissolved as $Sb(OH)_3$ and $Sb(OH)_2^+$ [42] while Sb_2O_5 dissolves as $HSb(OH)_6$ and $Sb(OH)_6^-$.

Wood [43] studied the Raman bands of a series of solutions of different Sb concentration at the same total sulphide concentration. A weak broad band at 314 cm^{-1}, a shoulder at 350 cm^{-1}, a sharper and more intense band at 369 cm^{-1}, and possibly another shoulder at about 380 cm^{-1} (all polarised) were observed in the 0.1 molal stock thioantimony solution prepared by dissolving Sb_2S_3 powder in the stock 1 molal Na_2S solution. The stock thioantimony solution was then diluted with the stock Na_2S solution in the ratios 3:2, 1:4, 0.5:4.5, and 0.25:4.75 and the Raman spectra recorded. In the first dilution bands at 314 and 350 cm^{-1} disappear while the bands at 369 and 380 cm^{-1} remain polarised and at the same intensity. No difference was observed in the second dilution apart from a decrease in overall intensity. For the third and fourth dilutions, Sb species is expected to be much less in concentration and thus harder to detect which necessitated the scan rate to be decreased considerably. A series of weak bands appeared at this point at 308, 338, and 448 cm^{-1} which the author attributed to minor amounts of oxidation products of sulphide such as polysulfide, polythionate, and thiosulphate. The bands at 369 and 380 cm^{-1} could still be seen at the third dilution although

weaker, but are too weak in the fourth. A calculation study by Tossell [41] later assigned the bands. Bands at 369 and 380 cm^{-1} are assigned to Sb-S stretch of the monomeric species $SbS_2(SH)^{2-}$ and $SbS(SH)_2^-$, 314 cm^{-1} to the Sb-SH stretch of the polymeric species $Sb_2S_2(SH)_2$, and 350 cm^{-1} to the Sb-S stretch of the same polymeric species. Tossell [42] also wrote that the calculated scaled symmetric stretch for $Sb(OH)_3$ should occur at 606 cm^{-1}.

Vibrational Spectroscopy of Sb_2O_3

Sb_4O_6 also possesses the cage unit. Beattie [25] reported Raman bands for powdered senarmontite at 87 (medium), 121 (weak – medium), 193 (medium – strong), 256 (very strong), 359 (very weak), 376 (weak – medium), 452 (medium), 717 cm^{-1} (weak). This author noted that there were large wavenumber differences between Sb_4O_6 and As_4O_6 fundamentals, which indicate a considerable force-field change between the two.

Senarmontite, cubic Sb_2O_3, showed Raman bands at 84, 124, 197, 261 (most intense), 364, 381, 458, and 722 cm^{-1} whereas valentinite, orthorhombic Sb_2O_3, had peaks at 71, 103, 140 (most intense), 194, 223, 269, 294, 449, 502, 602, 690 cm^{-1} [44]. The same study also reported the Raman spectrum of Sb_2O_3 glass to be almost identical with that of valentinite except that the lattice mode bands (under 400 cm^{-1}) are lost, indicating that the polymeric Sb-O chains are found in the melt as well. The above band positions were supported by later studies [45,46]. IR of senarmontite showed bands at 675 (shoulder), 740, and 960 cm^{-1} (weak) and valentinite at 455, 488 (shoulder), 540, 585 (shoulder), and 740 cm^{-1} [43]. The senarmontite band at 960 cm^{-1} was later shown to be unrelated to the ideal structure of the compound [46]. The IR spectrum of gaseous Sb_4O_6 has also been studied [47] and found that peak positions differ to those observed by Beattie [25] for Sb_4O_6 powder. Bands were observed at 785, 415, 292, and 175 cm^{-1}. The results agree more closely with those observed for senarmontite suspended in Nujol mulls in a study by Sourisseau and Mercier [48] at 744, 395, 272, and 179 cm^{-1}.

Quantum chemical simulation of both cubic and orthorhombic Sb_2O_3 had been performed using the GAMESS package at the density functional theory level with the B2LYP exchange-correlation potential [46]. Good agreement is observed between calculated and experimental data. The author concluded that the 750 – 300 cm^{-1} region corresponds to the

region of stretching vibration occurring in the chain plane, while the region below 300 cm^{-1} corresponds to deformation vibrations directed at angle to the chain plane.

For senarmontite, symmetric stretches of Sb-O-Sb were found at 465 (IR), 409 (IR), and 394 cm^{-1} (Raman), while the antisymmetric stretches were found at 765 (IR) and 574 cm^{-1} (IR). Its deformations lie at 282 (IR), 280 (Raman), 179 (Raman and IR), 126 (Raman), and 109 (Raman). For valentinite, there are two distinct bridging O atoms. Symmetric stretches of Sb-O1-Sb are found at 344 and 311 cm^{-1} (IR) and Sb-O2-Sb at 519 – 489 (Raman and IR) and 460 – 450 (Raman and IR) cm^{-1}. Antisymmetric stretches of O_1 are observed at 672 (IR), 663 (Raman and IR) cm^{-1}, and those of O2 at 600 – 550 (Raman and IR), 560 – 501 (IR) cm^{-1}. Bands from 316 – 200 cm^{-1} were determined to be a combination of scissoring, wagging, and twisting, of which are observed only in the Raman spectra with the exception of the twisting modes. Bands under ~160 cm^{-1} are assigned to lattice vibrations. Results are summarised in Table 10

Vibrational Spectroscopy of Sb_2O_4

$Sb^{3+}Sb^{5+}O_4$ exists as the orthorhombic α phase and a high temperature monoclinic β phase [44]. Both phases consist of corrugated sheets of Sb^{5+}-O octahedra running parallel to (001) linked by their corners, adjacent sheets are connected by Sb^{3+} ions. In the β phase the Sb^{3+} atom has 4 O atoms within bonding distance whereas the α phase there is a fifth O atom approaching Sb^{3+}.

The Raman spectra of the solid α phase have been reported to have bands at 75 (weak – medium), 91 (shoulder), 142 (weak), 200 (very strong), 221 (shoulder), 239 (weak), 255 (weak), 285 (shoulder), 400 (medium), 420 (medium), 467 (weak – medium), and a series of weak bands at 614, 652, 714, 758, and 825 cm^{-1} [44-45]. The β phase is produced by sealing the α phase in quartz capillaries to 960°C and leaving it for a few minutes [45]. The conversion mechanism is uncertain but is thought to be strongly influenced by the vapour pressure of the system. The pressure required for the formation of the β phase is approximately 5 atm. β-Sb_2O_4 gives rise to Raman bands at 79 (medium), 94 (weak – medium), 142 (weak), 195 (medium, shoulder), 212 (very strong), 283 (weak), 405 (medium), 439 (weak), and a series of weak bands at 466, 635, and 754 cm^{-1}. The IR spectrum of

α-Sb_2O_4 shows bands at 421, 528 (very weak), 605 (shoulder), 650, 745 cm^{-1} while β-Sb2O4 at 400 (shoulder), 420, 495 (shoulder), 625 (shoulder), 655, 715, 750 (shoulder) cm^{-1} [44-45].

The Raman spectrum of α-Sb_2O_4 nanorods has been published [49]. Peaks at 142, 195, and 259 cm^{-1} are assigned to O-Sb^{3+}-O vibration in the SbO4 tetragonal polyhedron, while those at 398 and 458 cm^{-1} are attributed to Sb^{3+}-O-Sb^{5+} (which connects SbO_4 and SbO_6 in the crystal). A weak band at 638 cm^{-1} is assigned to O-Sb^{5+}-O in SbO_6 octahedron. It's important to note that the Raman spectrum of nanorods displays small red shifts compared to bulk powders which may be due to a smaller size effect.

Preparation of Antimonites

Röhr [50] prepared alkali metal oxoantimonites of the structures $ASbO_2$ where A = K or Rb, and $A_4Sb_2O_5$ where A = K, Rb or Cs by reduction of Sb_2O_5, or of Sb_2O_3 and Sb_2O_5 with the alkali metal in a corundum crucible under Ar atmosphere at 500 – 600°C and afterwards cooled at a rate of 5 °C/hour. $KSbO_2$ was synthesised through conversion of elemental Sb with KO_2, while $RbSbO_2$ obtained through stoichiometric mixture of Rb, Sb_2O_3, and Sb_2O_5. $A_4Sb_2O_5$ is obtained by a stoichiometric mixture of Sb_2O_5 and the alkali metal. α-Sb_2O_4 nanorods [49] are synthesised by adding an analytically pure 0.004 mol of $SbCl_3$ and 0.0015 mol of I_2 into an autoclave of 50 mL capacity, which was then filled with distilled water up to 80% of total volume. The mixture is stirred for 5 minutes then the autoclave sealed and maintained at 200 °C for 20 hours. After cooling naturally to ambient temperature and washing the product with distilled water, the product is dried at 80 °C for 4 hours in a vacuum. Rutile structured $VSbO_4$ [51] was prepared by adding Sb_2O_3 powder to a red mixture previously made by adding V_2O_5 to a 3wt% H_2O_2 solution and stirred for about 25 minutes. The resulting mixture was refluxed for 3 hours to produce black slurry.

Orange lanthanum oxythioantimonite crystals [52] $La_6Sb_4O_{12}S_3$ was prepared from a mixture of La_2O_3, Sb_2S_3, and ZnO placed in a fused silica ampoule inside the glove box. The ampoule was flame sealed under vacuum and placed in a temperature-controlled tube furnace where it is heated to 1150°C over 30 hours and left for 7 hours. The cooling rate to ambient temperature was 4 °C/hour. Uranyl antimonite $UO_2Sb_2O_4$ [53] has been prepared from the hydrothermal reaction of UO_3 with Sb_2O_3 and KCl in a ratio of 1:1:2. The autoclave used has a 23 mL capacity, the volume of water that was added to the solids was 4 mL. The

autoclave was sealed, placed in a box furnace and heated to 180°C and held for 89 hours, after which the furnace was cooled at 9°C/hour to 23°C. The mother liquor is decanted from the products, which was then washed with water then methanol and dried. Even though neither K+ nor Cl- ions are present in the product, it is thought that Cl- acts as a mineraliser agent that aids in solubilising the UO_3 and in recrystallising the product. KCl can be substituted with CsCl. $MnSb_2O_4$ was prepared via hydrothermal synthesis [54] using stoichiometric mixtures of MnO and Sb_2O_3 in 5% HF solution. The reaction was carried out at 500°C and 1000 bars. The crystals are clear green in colour in the form of irregular needles.

Vibrational Spectroscopy of Synthetic Antimonites

Tabulated below are the results of Röhr [50]. The author notes that around 650 cm^{-1} a band will appear in compounds which have the 'open' Sb-O-Sb group, whereas a band around 614 cm^{-1} appears in the spectra of all compounds possessing the Sb-O-Sb group. $KSbO_2$ and $RbSbO_2$ crystallises isotypically as $CsSbO_2$. The characteristic building block of the structure is the stereochemically active lone pair of Sb^{3+} in the trigonal SbO_4 bipyramids, which are connected by their edges. $A_4Sb_2O_5$ where A = K, Rb, or Cs has the $[O_2Sb\text{-}O\text{-}Sb\text{-}O_2]^{4-}$ anion as building block, formed by two SbO_3 tetrahedra linked by a common bridging O. The K and Rb compounds have different conformations to the Cs compound.

Spectra of model $VSbO_4$ [51] catalysts with a cation defect gave rise to infrared and Raman bands at 460, 630, and 745 cm^{-1} which are assignable to rutile-related bulk stretching modes. According to X-ray diffraction data the fresh catalyst contains the $VSbO_4$ rutile phase, crystalline V_2O_5, and β-Sb_2O_4 phase. O-Sb-O vibrations are observed from 600 – 750 cm^{-1}. Symmetric and antisymmetric O-Sb-O stretches adjacent to the vacancy site would give rise to bands at 862 and 858 cm^{-1} respectively. $La_6Sb_4O_{12}S_3$ [52] consists of two different types of $[LaO_6S]$ polyhedra as the main building blocks together with $[Sb^{3+}O_3]$ tetrahedra. The $[SbO_3]$ polyhedra share an edge with two different types of $[LaO_6S]$ in the lattice. The author highlighted that the Raman spectrum reflects the $[Sb^{3+}O_3]^{3-}$ unit by presence of bands at 668, 438, 405, and 313. $[Sb^{3+}O_3]^{3-}$ has Cs symmetry.

The Raman and IR spectra of $MnSb_2O_4$ and $NiSb_2O_4$ have been published and the results tabulated below (Table 12) [54]. The results indicate that there are few differences above 300 cm^{-1} and that the cations only play a weak role in this region. The authors assigned Raman bands at 670 and 620 cm^{-1} to Sb-O bonds.

Synthesis of Antimonates

Antimonates of trirutile structure and of formula $M^{2+}Sb_2^{5+}O_6$ have been prepared by the thermal reaction of Sb_2O_3 with the metal oxide at 1050 °C for 50 hours [55]. Ilmenite-structured antimonates of formula M+SbO3 were prepared by Botto [56] by adding NaCl to a heated Sb_2O_3 solution, which will precipitate $Na[Sb(OH)_6]$. The product is then heated at 550°C for 3 to 4 hours which will result in $NaSbO_3$. At higher temperatures a perovskite structure is obtained instead. According to Siebert [57] the $M[Sb(OH)_6]$ needs to be heated to about 850°C to obtain $MSbO_3$. Antimonates with the $PbSb_2O_6$ type structure (where Pb can be substituted with Ca, Sr, Ba, Ag and Cd) are prepared by thermal reaction of Sb2O3 with the metal carbonate [58-61]. $Cd_2Sb_2O_7$ were prepared [60] by a reaction of Sb_2O_3 with CdO at 600 – 700 °C for 24 hours.

Vibrational Spectroscopy of Antimonates

Antimonates, like tantalates and niobates, of mono or divalent metals contain the MO_6 octahedra which can be assembled in different ways; they can link by their corners to form an ilmenite or perovskite structure, double octahedra M_2O_{10} linked by their apex to create layers of double octahedra whose structure is known as ‘block 1 x 2’ or to form chains oriented at 90° to one another to create a trirutile structure, double octahedral M_2O_{10} forming a ‘crown’ as in the structure known as $PbSb_2O_6$, or quadruple octahedral M_4O_{18} linked by their apex to form the columbite structure [62]. Farmer [63] also showed that a rutile XMO_4 structure is also known, formed by four O of the octahedra being shared giving a chain.

The M-O bonds can be differentiated into; terminal (1 O binds to 1 M and either 2 N^+ or 1 N^{2+} where N is the metal), bridging (1 O binds to 2 M and 1 N^+), or chain (1 O binds to 3 M). The bridging bonds are further classified into ordinary bonds, ring bonds, or bonds perpendicular to the double octahedral layer.

Husson [62] noted that for tantalates terminal bonds give rise to an intense band in the 910 – 840 cm^{-1} region. The region 890 – 750 cm^{-1} is occupied by a weak band corresponding to bridging bonds perpendicular to the double octahedral layer, while ordinary bridging bonds and ring bonds give rise to bands in the regions 770 – 500 cm^{-1} and 650 – 500 cm^{-1} respectively. The region corresponding to ordinary bridging bonds are rather wide; if the vibration propagates along the chain the band is expected towards 700 cm^{-1}, otherwise it is expected to occur towards 500 cm^{-1}. In the case of antimonates the bands are expected to occur at slightly higher wavenumbers than the above values.

The Raman and infrared spectra of trirutile antimonates $M^{2+}Sb_2^{5+}O_6$ where M = Zn, Mg, Co, Cu, and Ni have been published [55] and the results tabulated below. The minerals bystromite, $MgSb_2O_6$, and ordenezite, $ZnSb_2O_6$, have been studied by White [64], who showed that both compounds have two triplets above 400cm^{-1}. Bystromite showed the triplets at 785, 681, and 637 cm-1 and 604, 563, and 513 cm^{-1}, while ordonezite showed them at 794, 680, and 629 cm^{-1} and 585, 530, and 493 cm^{-1}. These results are in very close agreement with the results by Husson [55] presented below. $CuSb_2O_6$ has slightly different spectra to the other trirutile type compound, because it has a monoclinic distorted trirutile structure [65].

Sb-O bonds could either be simple bridging bonds Sb-O_b-Sb, or a ring (see fig) Sb-O_{cyc} each of which will manifest in the vibrational spectra.

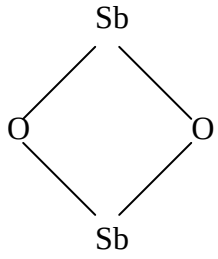

The Sb-O and M^{2+}-O bond lengths are very similar (1.97 – 2.01 Å and 2.01 – 2.06 Å respectively), and Husson [55] wrote that the M^{2+}-O vibrations should occur at a slightly lower wavenumber. However the M^{2+} atom does not take part in the structure, instead filling the vacant sites. Along the *c*-axis there are chains of octahedrons of the order Sb-Sb-M-Sb-Sb-M… connected to each other by their apexes. One chain is turned 90° to the other forming a basic plan of Sb_2O_{10} or double octahedrons. The author noted that vibrations of

$ZnSb_2O_6$ tend to occur at slightly lower wavenumbers compared to the other trirutile antimonates, which may be due to the lower electronegativity of Zn compared to Cu and Co.

The Raman spectra can be divided into regions which correspond to Sb-O_b-Sb vibrations (800 – 600 cm^{-1}), Sb-O_{cyc} vibrations (600 – 500 cm^{-1}), and Sb-Ob-Sb vibrations coupled with M-O vibrations and O-Sb-O angle deformation (500 – 400 cm^{-1}). In general the antisymmetric stretch if found at a higher wavenumber than the symmetric stretch. For $CoSb_2O_6$ and $MgSb_2O_6$ two bands near 740 cm^{-1} in Raman and near 700 cm^{-1} in infrared correspond to Sb-O_b-Sb. The splitting is due to the slightly inequivalent bond lengths.

Siebert [57] published infrared spectra of ilmenite-structured $NaSbO_3$ and the results were supported by Botto [56]. Furthermore Botto [56] used a CsI disk instead of KBr and was able to view down to about 150 cm^{-1}, and Raman data was also included. Siebert [57] states $NaSbO_3$ to show IR bands at 675 (medium), 637 (strong), 579 (very strong), and 527 cm^{-1} (strong) and $KSbO_3$ at 753 (weak), 646 (strong), 555 (very strong), 510 (strong), 476 (weak), and 420 cm^{-1} (weak). Botto [56] reports additional IR bands at 336 (strong), 232 (medium), and 179 cm^{-1} (medium), and Raman bands at 662 (medium – strong), 498 (weak – medium), 617 (weak), 315 (weak), 304 (weak – medium), 232 (weak), 205 (weak – medium), 158 (weak), and 118 cm^{-1} (weak).

Other antimonates analysed by Siebert [57] include $Na[Sb(OH)_6]$, $KSbO_3 \bullet 2.2H_2O$, $Na_2HSb_3O_9 \bullet 4H_2O$, and $K_2HSb_3O_9 \bullet 5H_2O$. Bands under 1000 cm^{-1} were assigned to Sb-O stretch, 1000 – 1200 cm^{-1} to Sb-OH bend, 2100 – 2350 cm^{-1} to the second overtone of Sb-OH bend, and 3220 – 3400 cm^{-1} to Sb-OH stretch and H_2O stretching vibrations. Botto [56] assigned bands below about 250 cm^{-1} to translation and rotation modes, symmetric stretch of Sb-O at 678 cm^{-1} and the antisymmetric stretch at 642 and 572 cm^{-1}, symmetric and antisymmetric deformation at 525 and 336 cm^{-1} respectively. Antimonates possessing the rutile structure $MSbO_4$ where M = Cr, Fe, Ga, and Rh were found to exhibit four IR bands at the 660 – 730 cm^{-1}, 520 – 585 cm^{-1}, 278 – 375 cm^{-1}, and 170 – 190 cm^{-1} [6] regions, and should have four Raman active bands as well although it has not been analysed using Raman spectroscopy.

Antimonates with the $PbSb_2O_6$-type structure contains SbO_6 octahedra linked by their edges forming a ‘crown’ of six octahedrons on the xy plane [58]. The crowns stack in the z

direction, linked by M^{2+}. The Sb-O bonds are of the cyclic nature, and every O atoms is bonded to 2 Sb and 1 M^{2+} atoms. Sb-O bond lengths are about 2 Å and Pb-O about 2.52 Å. Although the latter bond is long, it is thought to be strong since it assures the cohesion of the crystal. The authors note that the Pb-O vibrations may come up in higher wavenumbers.

If the samples are assumed to have a D_{3d} symmetry, they should have 6 Raman active bands ($2A_{1g}$ and 4_{Eg}) and 7 IR active bands ($3A_{2u}$ and $4E_u$). The profile of the spectra below 300 cm^{-1} differ between MSb_2O_6 where M = Pb, Ba, Sr, Cd, and Ca. Raman bands for $PbSb_2O_6$ were found at 670 (very strong), 510 (weak) , 498 (very weak), 318 (medium), 278 (weak), and 211 cm^{-1}(medium). Symmetric stretch of all the Sb-O bonds gives rise to the 670 cm^{-1} band, antisymmetric to 510 cm^{-1} (625 and 555 cm^{-1} in IR), symmetric bend at 498 cm^{-1} (476 cm^{-1} in IR), antisymmetric bend at 211 cm^{-1} (240 cm^{-1} in IR), and the rest being external modes (310, 117 and 86 cm^{-1} in IR).

Pyrochlore-structured antimonates ($Cd_2Nb_2O_7$) constitute SbO_6 octahedra linked by their apexes to form four hexagonal 'crowns', in the middle of which the divalent metal cation such as Cd^{2+} is found [60]. The cations receive a seventh O atom. The structure consists of a network of overlapping SbO_6 and Cd_4O (4 Cd^{2+} form a tetrahedron with an O at its centre. In the cubic unit cell containing eight molecules, 48 of 56 O atoms are coordinated to Sb. The SbO_6 octahedra have all of its O shared, whilst the remaining O are coordinated to M^{4+} or M^{2+}. Farmer [63] noted that interpretation of spectra of pyrochlore minerals can be difficult because there are many possibilities of replacement of both cations and anions, for example $M^{4+}Sb_2O_7$ can be substituted for $M^{2+}{}_2Sb_2O_7$. The Sb-O bonds are bridging ones, each O atom is linked to two Sb and two Cd atoms. The Cd atoms have two short Cd-O bonds and six longer Cd-O bonds. Pyrochlores of structures $A_2Sb_2O_6$ have the middle of the 'crowns' empty. For $A_2Sb_2O_7$ six Raman bands (A_{1g} and $4F_{2g}$) and seven IR bands ($7F_{1u}$) are expected, whereas compounds of formula $A_2Sb_2O_6$ is expected to show six Raman (A_{1g}, E_g, $2F_{1g}$, and $3F_{2g}$) and sixteen IR bands ($3A_{2u}$, $3E_u$, $6F_{1u}$, and $4F_{2u}$).

Since the IR band at 290 cm^{-1} observed in the spectrum of $Cd_2Sb_2O_7$ is absent in the $M_2Sb_2O_6$ spectrum, the authors deduced that this band must correspond to the vibration of the seventh O. $Na_2Sb_2O_6$ and $Ag_2Sb_2O_6$ IR spectra display bands at 720 (strong), 440 – 450 (strong), 330 – 350 (medium), 230 – 255 (medium), 120 (weak, only in $Na_2Sb_2O_6$), and 103 cm^{-1} (medium, only in $Ag_2Sb_2O_6$. $Cd_2Sb_2O_7$ shows IR bands at 760 (strong), 465 (strong),

360 (medium), 290 (medium), 230 (medium), 117 (weak), and 78 cm^{-1} (weak). $Ag_2Sb_2O_6$ shows Raman bands at 638 (medium, broad), 605 (strong), 480 (weak, shoulder), and 312 cm^{-1} (weak, sharp). The spectrum was not of excellent quality because of the noise. A Raman spectrum of sufficient quality of $Cd_2Sb_2O_7$ could not be obtained.

$Pb_2Sb_2O_7$, or a yellow pigment known as Naples yellow, is the isostructural anhydrous analogue of the mineral bindheimite $Pb_2Sb_2O_7(O,OH)$ [66-67]. There have been many Raman studies on Naples yellow [66-69], and the spectra show bands at 76 (strong), 147 (very strong), 343 (strong), 464 (medium), and 513 cm^{-1} (weak – medium) [66]. The band at 147 cm^{-1} is assigned to a lattice Pb-O stretch [66-67]. The spectrum by Kock [67] agrees fairly well with the above values, except that the band around 340 cm^{-1} is weak, and the band 76 cm^{-1} is not observed. A recent study by Miliani [59] shows a different spectrum; 107 (medium, sharp, with shoulders near 150 cm^{-1}), 190 (weak), 230 (medium), 298 (weak), 355 (weak), ~390 (weak), 423 (weak), 460 (shoulder, medium), 513 (strong), and 807 cm^{-1} (weak). The 510 cm^{-1} is assigned to the totally symmetric stretch of the SbO_6 octahedra, around 350 – 300 cm^{-1} to Sb-O and Pb-O bonds, under 300 cm^{-1} the bands are assigned to vibrations of Pb4O tetrahedral (lattice vibration of Pb and vibration of Pb with respect to the Sb-O sublattice). The authors also noted that Pb-O lattice mode varies from 125 to 150 cm^{-1}.

REFERENCES

[1] Greenwood, N. N., Earnshaw, A. (1997) *Chemistry of the Elements*, Pergamon, Oxford, UK

[2] Smith, J.D. *The Chemistry of Arsenic, Antimony, and Bismuth*

[3] Parkes, G.D. (1958) *Mellor's Modern Inorganic Chemistry,* Longmans, Green and Co., Bristol, UK

[4] Menary, J. W. (1958) The crystal structure of sodium polymetaarsenite $(NaAsO_2)_x$. *Acta. Cryst.*, 11: 742 – 743

[5] Norman, N. C. (1998) *Chemistry of Arsenic, Antimony, and Bismuth*, Blackie, London, UK

[6] Jensen, J. O., Gilliam, S. J., Banerjee, A., Zeroka, D., Kirkby, S. J. and Merrow, C. N. (2003) A theoretical study of As_4O_6: vibrational analysis, infrared and Raman spectra. *Theochem*, 664 – 665: 145 – 146

[7] Stranski, I. N., Plieth, K. and Zoll, I. (1958) The solution, solubility, and transitions of arsenolite and claudetite in water and aqueous solutions. *Zeit. Electrochem.*, 62: 366 – 372

[8] Pokrovski, G., Gout, R., Schott, J., Zotov, A. and Harrichoury, J. (1996) Thermodynamic properties and stoichiometry of As(III) hydroxide complexes at hydrothermal conditions. *Geochim. Cosmochim. Acta*, 60(5): 737 – 749

[9] Lee, C. and Harrison, W. T. A. (2004) The catena-arsenite chain anion, $[AsO_2]_n^{n-}$: $(H_3NCH_2CH_2NH_3)0.5[AsO_2]$ and $NaAsO_2$ (revisited) *Acta Cryst. Section C*, 60: 215 – 218

[10] Ghose, S., Boving, P., LaChappele, W. A. and Wan, C. (1977) Reinerite, $Zn_3(AsO_3)_2$: an arsenite with a novel type of zinc-tetrahedral double chain. *Am. Mineral.*, 62: 1129 – 1134

[11] Dunn, P. J., Peacor, D. R. and Darko Sturman, B. (1979) Paulmooreite, a new lead arsenite mineral from Langban, Sweden. *Am. Mineral.*, 64: 352 – 354

[12] Ghose, S., Sen Gupta, P. K. and Schlemper, E. O. (1987) Leiteite, $ZnAs_2O_4$: A novel type of tetrahedral layer structure with arsenite chains. *Am. Mineral.*, 72: 629 – 632

[13] Mellini, M. and Merlino, S. (1979) Versiliaite and apuanite: derivative structures related to schafarzikite. *Am. Mineral.*, 64: 1235 – 1242

[14] Nakamoto, K. (1986) *Infrared and Raman Spectra of Inorganic and Coordination Compounds*, John Wiley & Sons, Inc., New York, N.Y., U.S.A

[15] Wang, A., Han, J., Guo, L., Yu, J. and Zeng, P. (1994) Database of standard Raman spectra of minerals and related inorganic crystals. *App. Spectrosc.*, 48(8): 959 – 968

[16] Miller, F. A. and Wilkins, C. H. (1952) Infrared spectra and characteristic frequencies of inorganic ions. *Anal. Chem.*, 24(8): 1253 – 1294

[17] Bencivenni, L. and Gingerich, K. A. (1983) The characterisation of alkali arsenites and antimonites: the IR spectra of marix-isolated $MAsO_2$ and $MSbO_2$ molecules. *J. Mol. Structure*, 99: 23 – 29

[18] Ogden, J. S. and Williams, S. J. (1982) The characterisation of alkali metal phosphites, arsenites and antimonites. *J. Mol. Structure*, 80: 105 – 108

[19] Szymanski, H. A., Marabella, L., Hoke, J. and Harter, J. (1968) Infrared and Raman studies of arsenic compounds. *App. Spectrosc.*, 22(4): 297 – 304

[20] Loehr, T. M. and Plane, R. A. (1968) Raman spectra and structures of arsenious acid and arsenites in aqueous solution. *Inorg. Chem.*, 7(9): 1708 – 1714

[21] Falk, M. and Giguere, P. A. (1958) Infrared spectra and structure of selenious acid. *Canadian Journal of Chemistry*, 36: 1680 – 1685

923
924 [22] Tossell, J. A. (1997) Theoretical studies on arsenic oxide and hydroxide species in
925 minerals and in aqueous solution. *Geochim. et Cosmochim. Acta*, 61(8): 1613 – 1623
926
927 [23] Tossell, J. A. and Zimmermann, M. D. (2008) Calculation of the structures, stabilities,
928 and vibrational spectra of arsenites, thioarsenites and thioarsenates in aqueous solution.
929 *Geochim. et Cosmochim. Acta*, 72: 5232 – 5242
930
931 [24] Wood, S. A., Tait, C. D. and Janecky, D. R. (2002) A Raman spectroscopic study of
932 arsenite and thioarsenite species in aqueous solution at 25° C. *Geochem. Trans.*, 3(4):
933 31 – 39
934
935 [25] Akinfiev, N. N., Zotov, A. and Nikonorov, A. (1993) Thermodynamic analysis of
936 equilibria arsenic(III)-sulfur(II)-and oxygen-hydrogen. *Geochem. Int.*, 29: 109 – 121
937
938 [26] Beattie, I. R., Livingston, K. M. S., Ozin, G. A. and Reynolds, D. J. (1970) Single-
939 crystal Raman spectra of arsenolite (As_4O_6) and senarmontite (Sb_4O_6). The gas-phase
940 Raman spectra of P_4O_6, P_4O_{10}, and As_4O_6. *J. Chem. Soc.*, A: 449 – 451
941
942 [27] Lezal, D. and Konak, K. (1995) The characterization of the infrared absorption spectra
943 of the vitreous, cubic and monoclinic modification of As_2O_3. *J. Non-Crystal. Solids*,
944 192 – 193: 187 – 190
945
946 [28] Gilliam, S. J., Merrow, C. N., Kirkby, S. J., Jensen, J. O., Zeroka, D. and Banerjee, A.
947 (2003) Raman spectroscopy of arsenolite: crystalline cubic As_4O_6. *J. Solid State Chem*,
948 173: 54
949
950 [29] Brumbach, S. B. and Rosenblatt, G. M. (1972) In-cavity laser Raman spectroscopy of
951 vapors at elevated temperatures. As_4 and As_4O_6. *J. Chem. Phys.*, 56: 3110 – 3117
952
953 [30] Grzechnik, A. (1999) Compressibility and vibrational modes in solid As_4O_6. *J. Solid*
954 *State Chem.*, 144: 416 – 422
955

956 [31] Gout, R., Pokrovski, G., Schott, J. and Zwick, A. (1997) Raman spectroscopic study of
957 arsenic speciation in aqueous solutions up to 275° C. *J. Raman. Spectrosc.*, 28: 725 –
958 730
959
960 [32] Emmerling, F. and Röhr, C. (2003) Die neuen oxoarsenate(III) $AAsO_2$ (A = Na, K, Rb)
961 und $Cs_3As_5O_9$. Darstellung, kristallstrukturen und Raman-spektren. *Z. Naturforsch.*,
962 58B: 620 – 626
963
964 [33] Pertlik, F. (1988) The single chain arsenites $Pb(AsO_2)Cl$ and $Pb_2(AsO_2)_3Cl$. Preparation
965 and structure investigation. *Z. Kristallographie*, 184: 191 – 201
966
967 [34] Xiao, F., Zheng, Y., Wang, Y., Jian, H., Li, C., Xu, W. and Ma, Y. (2008) Preparation of
968 copper arsenite and its application in purification of copper electrolyte. *Trans.*
969 *Nonferrous Met. Soc. China*, 18: 474 – 479
970
971 [35] Pertlik, F. (1977) Zur synthese von kristallen von $CuAs_2O_4$ (trippkeit) und
972 $Cu_2As_3O_6CH_3COO$ (eine komponente des farbpigments Schweinfurter Grün). *Z. anorg.*
973 *Allg. Chem.*, 436: 201 – 206
974
975 [36] Curtin, L. P. (1927) Experiments in wood preservation. II – Arsenites of copper and zinc.
976 *Industrial and Engineering Chemistry*, 19(9): 993 – 999
977
978 [37] Avery, S. (1906) The constitutionof Paris Green and its homologues. *J. Am. Chem. Soc.*,
979 28: 1155 – 1164
980
981 [38] Subramanian, A., Vasudevan, T., Gnagadharan, R. and Raghavan, M. (2003) Solid state
982 synthesis of lithium meta arsenate. *US Patent Application 20030185745*
983
984 [39] Bell, I. M., Clark, R. J. H. and Gibbs, P. J. (1997) Raman spectroscopic library of
985 natural and synthetic pigments (pre- ~1850 AD). *Spectrochim. Acta Part A*, 53: 2159 –
986 2179
987
988 [40] Kloprogge, J. T. and Frost, R. L. (1999) Raman microscopy study of cafarsite. *App.*
989 *Spectrosc.*, 53(7): 874 – 88

[41] Zotov, A. V., Shikina, N. D. and Akinfiev, N. N. (2003) Thermodynamic properties of the Sb(III) hydroxide complex $Sb(OH)_{3(aq)}$ at hydrothermal conditions. *Geochim. et Cosmochim. Acta*, 67(10): 1821 – 1836

[42] Casas, J. M., Crisóstomo, G. and Cifuentes, L. (2004) Antimony solubility and speciation in aqueous sulphuric acid solutions at 298 K. *The Canadian Journal of Chemical Engineering*, 82: 175 – 183

[43] Tossell, J. A. (1994) The speciation of antimony in sulfidic solutions: a theoretical study. *Geochim. et Cosmochim. Acta*, 58(23): 5093 – 5104

[44] Wood, S. A. (1989) Raman spectroscopic determination of the speciation of ore metals in hydrothermal solutions: I. Speciation of antimony in alkaline sulphide solutions at 25° C. *Geochim. et Cosmochim. Acta*, **1989**, 53, 237 – 244

[45] Cody, C. A., DiCarlo, L. and Darlington, R. K. (1979) Vibrational and thermal study of antimony oxides. *Inorg. Chem.*, 18(6): 1572 – 1576

[46] Mestl, G., Ruiz, P., Delmon, B. and Knözinger, H. (1994) Sb_2O_3/Sb_2O_4 in reducing/oxidizing environments: an in situ Raman spectroscopic study. *J. Phys. Chem.*, 98: 11276 – 11282

[47] Voit, E. I., Panasenko, A. E. and Zemnukhova, L. A. (2009) Vibrational spectroscopic and quantum chemical study of antimony(III) oxide. *J .Struct.l Chem.*, 50(1): 60 – 66

[48] Konings, R. J. M., Booij, A. S. and Cordfunke, E. H. P. (1993) The infrared spectrum of gaseous antimony oxide (Sb_4O_6). *Chem. Phys. Lett.*, 210(4-6): 380 – 383

[49] Sourisseau, C. and Mercier, R. (1978) Vibrational spectra and calculation of the force field of arsenolite, senarmontite, and phosphorus oxide (P_4O_6). *Spectrochim. Acta A*, 34A(2): 173 – 178

[50] Gilliam, S. J., Jensen, J. O., Banerjee, A., Zeroka, D., Kirkby, S. J. and Merrow, C. N. (2004) *Spectrochim. Acta A.*, 60: 425 – 434

[51] Ren, G., Wang, C., Xia, J., Liu, J. and Zhong, H. (2009) Synthesis of α-Sb_2O_4 nanorods by a facile hydrothermal route. *Mat. Lett.*, 63: 605 – 607

[52] Hirschle, C. and Röhr, C. (2000) Alkalimetall-oxoantimonate: synthesen, kristallstrukturen und schwingungsspektren von $ASbO_2$ (A = K, Rb), $A_4Sb_2O_5$ (A = K, Rb, Cs) und Cs_3SbO_4. *Z. Anorg. Allg. Chem.*, 626: 1305 – 1312

[53] Stair, P. C., Xiong, G., Sullivan, V. S., Zajac, G. W., Trail, S. S., Kaduk, J. A., Golab, J. T. and Brazdil, J. F. (2005) Effect of titanium substitution on the structure of $VSbO_4$ catalysts for propane ammoxidation. *J. Catalysis*, 230: 317 – 326

[54] Dorhout, P. K., So, W., LaCour, A. and Aliev, V. O. (2004) Synthesis and characterization of a new quarternary lanthanum oxythioantimonite: $La_6Sb_4O_{12}S_3$. *J. Alloys and Compounds*, 374: 234 – 239

[54] Albrecht-Schmitt, T. E., Sykora, R. E., King, J. E. and Illies, A. J. (2004) Hydrothermal synthesis, structure, and catalytic properties of $UO_2Sb_2O_4$. *J. Solid State Chem.*, 177: 1717 – 1722

[56] Chater, R., Gavarri, J. R. and Genet, F. (1986) Composes isomorphes $MeX_2O_4E_2$. I. Etude vibrationelle de $MnSb_2O_4$ entre 4 et 300 K: champ de force et tenseur élastique. *J. Solid State Chem.*, 63: 295 – 307

[57] Sejkora, J., Ozdin, D., Vitalos, J., Tucek, P., Cejka, J. and Duda, R. (2007) Schafarzikite from the type locality Pernek (Malé Karpaty mountains, Slovak Republic) revisited. *Eur. J. Mineral*, 19: 419 – 427

[58] Husson, E., Repelin, Y. and Brusset, H. (1979) Spectres de vibration et calcul du champ de force des antimoniates et des tantalates de structure trirutile. *Spectrochim. Acta*, 35A: 1177 – 1187

[59] Baran, E. J. and Botto, I. L. (1981) Espectro vibracional del $NaSbO_3$. *Anales Asoc. Quim. Argentina*, 69: 283 – 291

[60] Siebert, H. (1959) Ultrarotspektren von tellursäuren, telluraten und antimonaten. *Z. Anorg. Allg. Chem.*, 301: 161 – 170

[61] Vandenborre, M. T., Husson, E. and Brusset, H. (1980) Spectres de vibration et calcul du champ de force des antimoniates de structure 'type $PbSb_2O_6$'. *Spectrochim. Acta,* 36A: 1045 – 1052

[62] Magneli, A., (1941) The crystal structure of $PbSb_2O_6$ and isomorphous compounds. *Arkiv. Kemi. Miner. Geol.,* 15B(3): 1 – 6

[63] Vandenborre, M. T., Husson, E. and Fourquet, J. L. (1982) Spectres vibrationnels et champ de force de divers composes de formule $A_2B_2O_7$ et $A_2B_2O_6$ de structure pyrochlore. *Spectrochim. Acta,* 38A(9): 997 – 1003

[64] Husson, E., Repelin, Y. and Vandenborre, M. T. (1984) Spectres de vibration et champ de force de l'antimoniate et de l'arseniate de calcium $CaSb_2O_6$ et $CaAs_2O_6$. *Spectrochim. Acta,* 40A(11 – 12): 1017 – 1020

[65] Husson, E., Repelin, Y. and Nguyen, Q. D. (1980) Etude vibrationelle de divers niobates, tantalates et antimoniates. *Conf. Int. Spectrosc. Raman, 7th*, 194 – 195

[66] Farmer, V. C. (1974) *The Infrared Spectra of Minerals*, Mineralogical Society, London, UK

[67] White, W. B., (1967) Application of IR spectroscopy to order-disorder problems in simple ionic solids. *Mater. Res. Bull.,* 2: 381 – 394

[68] Byström, A., Brita, H. and Mason, B. (1942) The crystal structure of zinc meta antimonate and similar compounds. *Ark. Kemi. Mineral. Geol.*, 15B(4): 1 – 8

[69] Clark, R. J. H., Cridland, L., Kariuki, B. M., Harris, H. D. M. and Withnall, R. (1995) Synthesis, structural characterisation and Raman spectroscopy of the inorganic pigments lead tin yellow types I and II and lead antimonite yellow: their identification on medieval paintings and manuscripts. *J. Chem. Soc. Dalton Trans.*, 16: 2577 – 2582

[70] Kock, L. D. and De Waal, D. (2008) Raman analysis of ancient pigments on a tile from the Citadel of Algiers. *Spectrochim. Acta Part A*, 71: 1348 – 1354

[71] Edwards, H. G. M., Domenech-Carbo, M. T., Hargreaves, M. D. and Domenech-Carbo, A. (2008) A Raman spectroscopic and combined analytical approach to the restoration of severely damaged frescoes: the Palomino project. *J. Raman Spectrosc.*, 38: 444 – 452

[72] Miliani, C., Rosi, F., Manuali, V., Brunetti, B. G., Sgamellotti, A., Grygar, T. and Hradil, D. (2009) Raman scattering features of lead pyroantimonate compounds. Part I: XRD and Raman characterization of $Pb_2Sb_2O_7$ doped with tin and zinc. *J. Raman Spectrosc.*, 40: 107 – 111

List of Tables